



Published in final edited form as:

*Opt Mater Express*. 2018 July 1; 8(7): 2017–2025. doi:10.1364/ome.8.002017.

## Dynamic optical response of SU-8 upon UV treatment

Alok Ghanekar<sup>1</sup>, Matthew Ricci<sup>2</sup>, Yanpei Tian<sup>1</sup>, Otto Gregory<sup>2</sup>, Yi Zheng<sup>1,\*</sup>

<sup>1</sup>Department of Mechanical, Industrial and Systems Engineering, University of Rhode Island, Kingston, RI 02881, USA

<sup>2</sup>Department of Chemical Engineering, University of Rhode Island, Kingston, RI 02881, USA

### Abstract

We report the optical properties of SU-8 in the mid-infrared (mid-IR) region before and after UV treatment. Samples consisted of SU-8 films of thickness ranging from 10  $\mu\text{m}$  to 157  $\mu\text{m}$  deposited on gold coated silicon substrates and were prepared using spin coating. Mid-IR diffuse reflectance measurements were conducted using Fourier transform infrared spectroscopy. Spectra measurements imply a change in optical properties of SU-8 upon exposure to UV and heat treatment. A gradual change in optical properties is seen after each step of UV treatment and the baking process. Reflectance spectra of thin-films were also observed to be thickness dependent. We calculate the dielectric function of SU-8 in the range 2  $\mu\text{m}$  to 15  $\mu\text{m}$  using the reflectance spectra of the samples.

### 1. Introduction

Continuous development in lithography and micromachining has led to invention of a photoresist known as SU-8 by IBM research [1, 2]. SU-8 is a photosensitive epoxy polymer that is now commonly used as negative photoresist for optical lithography, especially for high-aspect ratio lithography [3]. SU-8 has been shown compatible with other nanoscale lithography techniques, such as electron beam lithography and x-ray lithography [4]. SU-8 is of prime importance in fabrication of semiconductor devices, micro-electromechanical systems (MEMS) and microfluidics [5]. Due to its bio-compatibility, SU-8 is also used for bio-MEMS applications [6]. Owing to its good thermal stability and young's modulus, SU-8 can be potentially used for nanoimprint lithography [7]. When exposed to ultraviolet (UV) light, SU-8 undergoes cross-linking leading to polymerization, making it insoluble in solvents such as Acetone, Methyl Ethyl Ketone (MEK) or N-Methyl Pyrrolidinone [2]. While optical properties of SU-8 in visible and UV range have been characterized [8], infrared refractive indices of SU-8 were not estimated until recently [9]. Fourier Transform Infrared Spectroscopy (FTIR) measurements using attenuated total reflectance (ATR) method have also been documented before and various IR absorption bands have been assigned to several different functional groups [10–12]. Mid-IR dielectric function of SU-8 was first reported by Motaharifar et al. [9] using reflection and transmission spectra of a free-standing SU-8 sample. Here, we calculate dielectric function of SU-8 using reflectance

\* zheng@uri.edu.

data for various thickness of SU-8 films. We also observe its reflectance spectra before and after UV treatment.

Polymers in general have been investigated for possible selective thermal emission properties [13]. They can also be embedded with nanoparticles furthering spectral control of thermal emission [14–17]. Infrared spectral response of polydimethylsiloxane (PDMS) [13], poly(vinyl chloride) (PVC) [18], poly(vinyl fluoride) (PVF) [19] and poly(4-methyl-1-pentene) (PMP) [20] have been studied before. It would be crucial to study spectral response of SU-8 thin films in the infrared region, especially given its sensitivity to UV treatment. We report the optical response of SU-8 in mid-infrared (mid-IR) region: 2  $\mu\text{m}$  to 15  $\mu\text{m}$ . Here, mid-IR optical response of SU-8 thin films have been reported before and after UV treatment. Based on the reflectance spectra of thin films of various thicknesses of SU-8, we have calculated its dielectric function using extended Lorentz model.

The main constituents of the SU-8 photoresists are the EPON Resin SU-8 (Shell Chemical) and triarylsulfonium hexafluoroantimonate salt (CYRACURE UVI, Union Carbide) photoacid generator that makes it photosensitive to UV light at 310 and 230 nm [21]. UV exposure causes hexafluoroantimonate salt to decompose to form hexafluoroantimonic acid that in turn protonates the EPON oligomer. These protonated ions react with epoxides in cross-linking reactions upon heating (baking) [21]. Therefore, UV exposure of SU-8 pattern is usually followed by a few baking steps during optical photolithography. In this work, we prepared several samples of SU-8 thin films of various thickness coated on a reflecting layer of gold over silicon wafers and recorded the reflectance spectra of the samples after each step that would normally be undertaken during optical lithography. Reflectance spectra of samples with various thicknesses are used to estimate refractive indices of the polymer in the mid-IR region.

## 2. Sample preparation

Silicon (Si) wafers were cleaned using successive washes of acetone, methanol and deionized water and dried using nitrogen gas. The wafers were then heated to 120 °C on a hot plate to release adsorbed gases. 2  $\mu\text{m}$  of 4N gold were deposited on the smooth side of the Si wafer using RF sputtering via an MRC 8667 RF Sputtering Machine in 9 mTorr argon gas. Various thicknesses of SU-8 3005 were spin coated onto the gold coated substrates using a Laurell Technologies WS-400 Spin Coater. Soft baking, exposure, post exposure baking and hard baking were performed according to procedures suggested by the manufacturer and heated using a Fischer Scientific Isotemp hotplate (see Fig. 1 for schematic). UV Exposure was performed using an OAI UV Exposure and Aligner workstation. Photoresist thicknesses were confirmed using a Dektak II stylus profilometer.

## 3. Reflectance measurements

Reflection spectra of the prepared samples were measured using Jasco 6600 FTIR spectrometer equipped with PIKE's diffuse reflectance accessory known as mid-IR integrated sphere. The spectrometer has a ceramic source that radiates IR light while the integrated sphere uses its own dedicated mercury cadmium telluride (MCT) detector. The

source and the detector allow measurements in the range 2  $\mu\text{m}$  to 15  $\mu\text{m}$  with sufficient accuracy. Sample is placed on the the top of the accessory facing downwards. The accessory has a spherical shell coated with a highly reflective layer of gold. The IR light from the interferometer falls on the sample via a gold mirror. Light scattered by the sample is collected by the gold sphere and is eventually captured by the MCT detector. The central mirror can be turned to point at the sphere to take reference measurement of gold (assumed to be 100% reflecting). Angle of incidence on the sample is fixed to 12  $^\circ$ . Nearly 96% of the reflection is specular while about 4% is diffuse. This highlights the quality of the samples. As all scattered light is collected, measured reflectance ( $r$ ) can be directly related to absorbance ( $a$ ) by  $a = 1 - r$ . Each measurement consists of a background measurement and a sample measurement. Scan rate was set to 64 scans per measurement with a resolution of 0.4  $\text{cm}^{-1}$ . Three measurements were taken for each sample from different location on the sample. Repeated measurements at different locations were found to be essentially same; this also confirms the quality of the samples.

## 4. Results and discussion

### 4.1. Reflectance spectra

Four samples of SU-8 thin films of thicknesses 10  $\mu\text{m}$ , 20  $\mu\text{m}$ , 50  $\mu\text{m}$  and 157  $\mu\text{m}$  coated on a gold substrate were prepared (hereafter we will refer to samples as thin films). This was followed by standard processing steps during optical lithography: soft baking (Stage I), UV exposure (Stage II), post-exposure bake (Stage III) and hard bake (Stage IV). For the 10  $\mu\text{m}$  sample, reflectance measurement were recorded at each stage as shown Fig. 2(a). As the thickness of the gold layer is much larger than the penetration depth ( $\lambda/4\pi\kappa$ ) of mid-IR radiation, it is thick enough to be opaque. The layer of gold is also highly reflecting (>98%) for the range of wavelengths considered here. Therefore, the spectra show optical properties of SU-8. Reflectance spectrum shows several absorption bands. Each of the absorption bands relate to a specific chemical bond. FTIR spectroscopy using attenuated total reflection (ATR) mode is often performed to identify different chemical bonds in the samples [12]. Here, we have conducted diffuse reflectance measurements instead. While diffuse reflectance spectroscopy is more quantitative than ATR method, the spectrum does not necessarily display all the distinct absorption bands. However, some typical absorptions peaks are clearly visible in the thin-film reflectance spectrum that we briefly discuss. The most notable peaks are due to O-H stretch around 3200-3500  $\text{cm}^{-1}$  ( $\sim 3 \mu\text{m}$ ), aromatic C-H stretch at 3050  $\text{cm}^{-1}$  ( $\sim 3.3 \mu\text{m}$ ) and aliphatic C-H stretch around 2960-2870  $\text{cm}^{-1}$  ( $\sim 3.45 \mu\text{m}$ ). In addition, peaks corresponding to aliphatic  $\text{CH}_3$  bending ( $\sim 1390 \text{ cm}^{-1}$ ; 7.2  $\mu\text{m}$ ),  $\text{CH}_2$  bending ( $\sim 1540 \text{ cm}^{-1}$ ; 6.5  $\mu\text{m}$ ), and aromatic C-C stretching ( $\sim 1724 \text{ cm}^{-1}$ ; 5.8  $\mu\text{m}$ ) are also observed. This denotes presence of alkyl and aryl groups present in SU-8.

A change in reflectance spectrum is seen after each stage of treatment, more prominent changes are seen at specific wavelength bands, while some parts of spectrum are unchanged. The UV exposure step induces the greatest change in the reflectance spectrum. Absorption band near 3  $\mu\text{m}$  shows prominent increase in absorption upon UV exposure. This is the band corresponding to O-H stretch. Increase in absorption in this region suggests an increased number of hydroxyl (O-H) groups through crosslinking of epoxy groups in SU-8. At longer

wavelengths (10 to 15  $\mu\text{m}$ ), it is difficult to assign the change in spectrum to particular bonds. However, this is the region where absorption bands corresponding to aromatic C-H bends lie [10]. Being an epoxy, SU-8 layers are sticky, especially for thicker films. Hence it was not possible to conduct reflectance measurements for the thicker films before UV exposure (as they tend to stick to the apparatus). However, after UV exposure and baking stages, SU-8 becomes completely dry and measurements can be taken.

Figure 2(b) shows reflectance spectra of UV exposed and baked samples of SU-8 of various thicknesses: 10  $\mu\text{m}$ , 20  $\mu\text{m}$ , 50  $\mu\text{m}$  and 157  $\mu\text{m}$ , respectively. A gradual reduction in reflectance was observed as the thickness of the films increases. While thinner films show absorption at several bands, thicker samples display a broader absorption throughout the infrared region. Appearance of several sharp peaks in the thin film spectra is due to surface phonon modes [22] corresponding various modes of vibrations. Absorption peaks in thin-film spectra can be related to refractive indices of the material [22].

#### 4.2. Estimation of dielectric function

To estimate the dielectric function of SU-8, we use the method outlined by Verleur et al. [23]. Inspired by Srinivasan's [13] approach to calculate dielectric function of PDMS, we employ a similar process to calculate dielectric function of SU-8. We picked reflectance measurements of all samples to extract the dielectric function. Dielectric function  $\epsilon(\omega)$  of a polymer can be assumed to be of Lorentz-Drude oscillator form given by [23],

$$\epsilon(\omega) = \epsilon_{\infty} + \sum_{k=1}^N \frac{s_k}{1 - \left(\frac{\omega}{\omega_k}\right)^2 - j\Gamma_k\left(\frac{\omega}{\omega_k}\right)}. \quad (1)$$

Here,  $s_k$ ,  $\omega_k$ ,  $\Gamma_k$  and  $j$  are the strength, resonant frequency, damping factor of  $k$ th Lorentz-Drude oscillator and the imaginary unit, respectively.  $N$  such oscillators are assumed.  $\epsilon_{\infty}$  is the contribution from higher frequencies. Since the angle of incidence in the measurements is  $12^\circ$ , reflectance values were calculated for that angle of incidence.  $\omega_k$  correspond to several of the vibrational bond resonances inside the material. High absorption and strong dispersion exist around these resonance frequencies.

For an unpolarized incident beam of light, reflectance  $r_c$  for any angle of incidence is related to polarized reflection coefficients by [24]

$$r_c = \frac{1}{2} [ |R^{TE}|^2 + |R^{TM}|^2 ] \quad (2)$$

Here,  $R^{TE}$  and  $R^{TM}$  are effective reflection coefficients at the given angle of incidence for transverse electric (TE) and transverse magnetic (TM) polarization, respectively.

Consider a structure having 3-layer media: air, SU-8 and gold, respectively. Substrate below the gold layer can be ignored as gold is assumed to be 100% reflective. By solving the boundary conditions at the interfaces, one can obtain the expression for the generalized (or effective) reflection coefficient at the air-SU-8 interface which is given by [24],

$$R^{(\mu)} = \frac{R_{12}^{(\mu)} + R_{23}^{(\mu)} e^{2jk_{2z}L}}{1 + R_{12}^{(\mu)} R_{23}^{(\mu)} e^{2jk_{2z}L}} \quad (3)$$

where  $R_{12}^{(\mu)}$  is the Fresnel reflection coefficient at the interface between the layer 1 and 2, and  $R_{23}^{(\mu)}$  is the Fresnel reflection coefficient at the interface between the layer 2 and 3,  $\mu = s$  (or  $p$ ) refers to TE (or TM) polarization,  $L$  is the thickness of SU-8 layer. Since we are dealing with an oblique angle of incidence ( $12^\circ$ ),  $k_{2z} = \sqrt{\epsilon(\omega)\omega^2 / c^2 - k_p^2}$  is the normal component of the wave vector in SU-8 wherein  $\epsilon(\omega)$  is the relative permittivity of SU-8 as a function of angular frequency  $\omega$ ,  $c$  is the speed of light in vacuum and  $k_p = \sin(12^\circ)\omega/c$  is the magnitude of the in-plane wave vector. The above expression accounts for multiple reflections and inventual absorption within the SU-8 layer and it is valid for thin as well as bulk SU-8 coated on gold.

Dielectric function of SU-8 was obtained by tuning several oscillator parameters by matching reflectance spectra of both thin films and bulk samples. This involved an optimization procedure that aims to minimize the error between calculated and measured spectra. The error between the spectra is given by

$$\delta = \sum_{i=1}^M [r_m - r_c]^2 \Big|_{10 \mu m} + \sum_{i=1}^M [r_m - r_c]^2 \Big|_{20 \mu m} + \sum_{i=1}^M [r_m - r_c]^2 \Big|_{50 \mu m} + \sum_{i=1}^M [r_m - r_c]^2 \Big|_{157 \mu m} \quad (4)$$

Here,  $r_m$  and  $r_c$  are measured and calculated values of reflectance, respectively. Index  $i$  refers to  $M$  different frequencies over which the measurements are taken. One may use reduced Chi-Squared function instead of using absolute error squared as an objective function. One of the issues with reduced Chi-Squared function is that, it produces large values for low reflectance points. This gives higher weightage to thicker samples (because they have very low reflectance on an average). As a result, it produces a good fit for thick samples but not for films. This method is not practical when dealing with samples of various thicknesses. Therefore, absolute error squared was used as objective function.

The minimization was done in two steps. In the first step, we used MATLAB based genetic algorithm to arrive at an initial guess of oscillator parameters. This brings us closer to the global optimum of the objective function, providing a reasonable fit. This is further improved by using constrained optimization function *fmincon*. It was found that eighteen such resonant frequencies are needed to achieve a good fit with the experimental data. As observed by Verleur [23], at least one oscillator mode is needed to be outside the spectral range of measurement to achieve a good fit. In our case, this is located at  $15.4 \mu m$ . The oscillator parameters for the UV exposed and heat treated SU-8 are provided in Table 1. Infrared refractive indices calculated using reflectance measurements of UV exposed and heat treated SU-8 samples are shown in Fig. 3. Comparison of measured and calculated

reflectance of UV treated SU-8 samples are shown in Fig. 4. Although thicker samples of unexposed SU-8 could not be used for measurements, thin film measurements of unexposed SU-8 samples (10  $\mu\text{m}$ ) and measurements of exposed SU-8 samples with 50  $\mu\text{m}$  and 157  $\mu\text{m}$  thickness were used to estimate dielectric function of unexposed SU-8 and its parameters are tabulated in Table 2. While resonant frequencies of the dielectric function of SU-8 are very similar before and after exposure, values of oscillator strength parameters and damping factors are different. Some of the resonant frequencies can be related to well-known IR absorption bands that are associated with typical chemical bonds in organic materials. Those are also listed in the tables for the reader's convenience. In the recent work, Motaharifar et al. [9] estimated dielectric function of UV and heat treated SU-8. Their model identifies only six resonance frequencies that are also similar to the frequencies identified in this work. These frequencies are 24.3 (24.7), 30.6 (32), 33.4 (32), 35.3 (36.8), 36.7 (36.8) and 45.0 (44.4) THz. Here, the numbers in the bracket denote resonance frequencies estimated in the present work.

Average error between calculated and reflected spectra is about 5%. Given that the estimated dielectric function allows us to calculate and match reflectance curves for four different film thicknesses, such an error is reasonable. In Fig. 4, we observe that reflectance curves of thicker samples of SU-8 show flat regions. Such a response cannot be a result of Lorentzian model as clearly seen from the deviations in spectrum for thicker films, e.g. 157  $\mu\text{m}$  sample. However, it does not mean that Lorentz-Drude model is invalid for SU-8. We account for such differences to the errors in reflectance measurements for thicker samples. Uncertainties in reflectivity measurements for thick samples can be larger due to their low reflectance. As the reference standard is 100% reflectance, measured signal for highly absorbing (weakly reflecting) samples is small and contains more noise. As a result, some features of the reflectance spectra are lost. However, the reflectance data from these thicker samples is necessary for correct estimation of  $\epsilon_{\infty}$ . We also observed that thicker samples tend to have non-uniformity issues. Moreover, there are difficulties in fabricating bulk samples that do not crack or display wrinkling on the surface. For this reason, we did not include bulk samples measurements of SU-8 for estimation of dielectric function.

## 5. Conclusion

In summary, we have reported optical properties of SU-8 using FTIR diffuse reflectance spectroscopy. Observations were made before and after UV treatment of the samples. Reflectance spectra clearly show change standard steps of UV exposure and heat treatment are followed. Reflectance spectra of the polymer is thickness-dependent. Reflectance spectra of various thicknesses can be used to estimate dielectric function of the polymer that obeys Lorentz-Drude oscillator model. The oscillator parameters for the dielectric function were identified using a curve fitting optimization routine between predicted and simulated reflectance spectra.

## Acknowledgments

This project was supported in part by a National Science Foundation through grant number 1655221, Institutional Development Award (IDeA) Network for Biomedical Research Excellence from the National Institute of General Medical Sciences of the National Institutes of Health under grant number P20GM103430, and Rhode Island

Foundation Research Grant number 20164342. Authors would like to thank Dr. Bharathy Subramanian Parimalam for his comments on chemical aspects of SU-8.

#### Funding

National Science Foundation (1655221); Institutional Development Award (IDeA) Network for Biomedical Research Excellence from the National Institute of General Medical Sciences of the National Institutes of Health under (P20GM103430); Rhode Island Foundation Research (20164342).

## References and links

1. LaBianca NC and Gelorme JD, "High-aspect-ratio resist for thick-film applications," in SPIE's 1995 Symposium on Microlithography (International Society for Optics and Photonics, 1995), pp. 846–852.
2. Lorenz H, Laudon M, and Renaud P, "Mechanical characterization of a new high-aspect-ratio near UV-photoresist," *Microelectron. Eng* 41, 371–374 (1998).
3. "<http://www.microchem.com/prod-su8.htm>,".
4. del Campo A and Greiner C, "Su-8: a photoresist for high-aspect-ratio and 3d submicron lithography," *J. Micromechanics Microengineering* 17, R81 (2007).
5. Zhang J, Tan K, Hong G, Yang L, and Gong H, "Polymerization optimization of su-8 photoresist and its applications in microfluidic systems and mems," *J. Micromechanics Microengineering* 11, 20 (2001).
6. Nemani KV, Moodie KL, Brennick JB, Su A, and Gimi B, "In vitro and in vivo evaluation of su-8 biocompatibility," *Materials Science and Engineering: C* 33, 4453–4459 (2013). [PubMed: 23910365]
7. Sua J, Gaob F, Gub Z, Daic W, Cernigliaroc G, and Sun H, "Fabrication of su-8 based nanopatterns and their use as a nanoimprint mold," *Proc. SPIE* 8974, 897409 (2014).
8. Parida OP and Bhat N, "Characterization of optical properties of su-8 and fabrication of optical components," in *Int. Conf. on Opt. and Photon.(CSIO)* (2009), pp. 4–7.
9. Motaharifar E, Pierce R, Islam R, Henderson R, Hsu J, and Lee M, "Broadband terahertz refraction index dispersion and loss of polymeric dielectric substrate and packaging materials," *Journal of Infrared, Millimeter, and Terahertz Waves* 39, 93–104 (2018).
10. Tan T, Wong D, Lee P, Rawat R, and Patran A, "Study of a chemically amplified resist for x-ray lithography by fourier transform infrared spectroscopy," *Appl. Spectrosc* 58, 1288–1294 (2004). [PubMed: 18070406]
11. Smith BC, *Infrared Spectral Interpretation: A Systematic Approach* (CRC Press, 1998).
12. Wang X-B, Sun J, Chen C-M, Sun X-Q, Wang F, and Zhang D-M, "Thermal uv treatment on su-8 polymer for integrated optics," *Opt. Mater. Express* 4, 509–517 (2014).
13. Srinivasan A, Czaplá B, Mayo J, and Narayanaswamy A, "Infrared dielectric function of polydimethylsiloxane and selective emission behavior," *Appl. Phys. Lett* 109, 061905 (2016).
14. Gentle AR and Smith GB, "Radiative heat pumping from the earth using surface phonon resonant nanoparticles," *Nano Lett.* 10, 373–379 (2010). [PubMed: 20055479]
15. Smith G, Deller C, Swift P, Gentle A, Garrett P, and Fisher W, "Nanoparticle-doped polymer foils for use in solar control glazing," *Journal of Nanoparticle Research* 4, 157–165 (2002).
16. Heilmann A, *Polymer Films with Embedded Metal Nanoparticles*, vol. 52 (Springer Science & Business Media, 2013).
17. Ghanekar A, Lin L, Su J, Sun H, and Zheng Y, "Role of nanoparticles in wavelength selectivity of multilayered structures in the far-field and near-field regimes," *Opt. Express* 23, A1129–A1139 (2015). [PubMed: 26406743]
18. Felix T, "Devices for lowering the temperature of a body by heat radiation therefrom" US Patent 3,310,102 (1967).
19. Bartoli B, Catalanotti S, Coluzzi B, Cuomo V, Silvestrini V, and Troise G, "Nocturnal and diurnal performances of selective radiators," *Appl. Energy* 3, 267–286 (1977).
20. Grenier P, "Radiative cooling-inverse greenhouse effect," *Revue de Physique Appliquee* 14, 87–90 (1979).

21. Teh W, Dürig U, Drechsler U, Smith C, and Güntherodt H-J, "Effect of low numerical-aperture femtosecond two-photon absorption on (SU-8) resist for ultrahigh-aspect-ratio microstereolithography," *J. Appl. Phys* 97, 054907 (2005).
22. Narayanaswamy A, Mayo J, and Canetta C, "Infrared selective emitters with thin films of polar materials," *Appl. Phys. Lett* 104, 183107 (2014).
23. Verleur HW, "Determination of optical constants from reflectance or transmittance measurements on bulk crystals or thin films," *JOSA* 58, 1356–1364 (1968).
24. Chew WC, *Waves and Fields in Inhomogeneous Media* (IEEE Press, 1995).

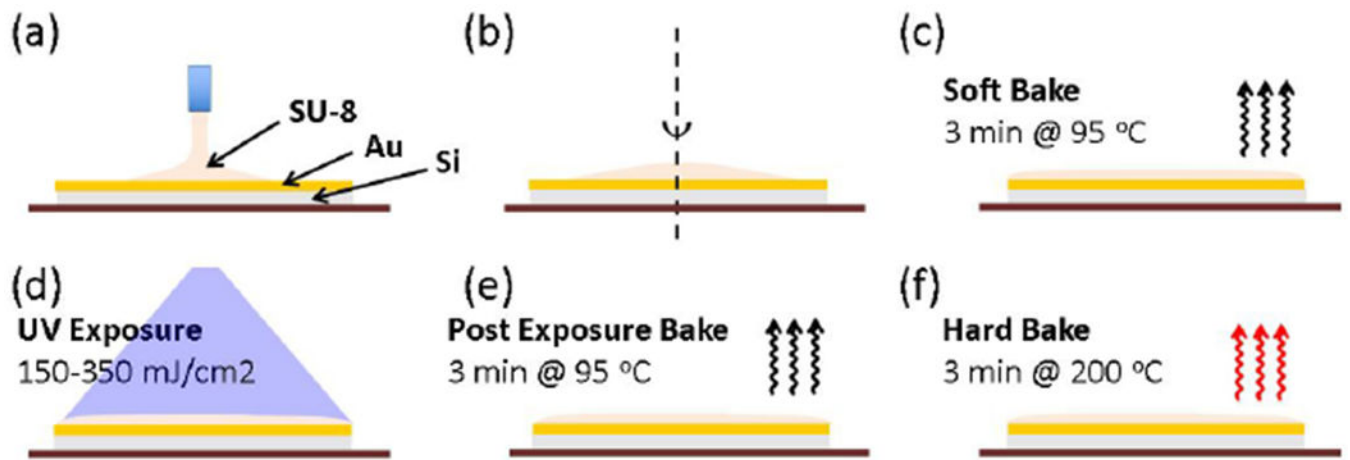


**Fig. 1.** Schematic of sample preparation, UV exposure and heat treatment steps.

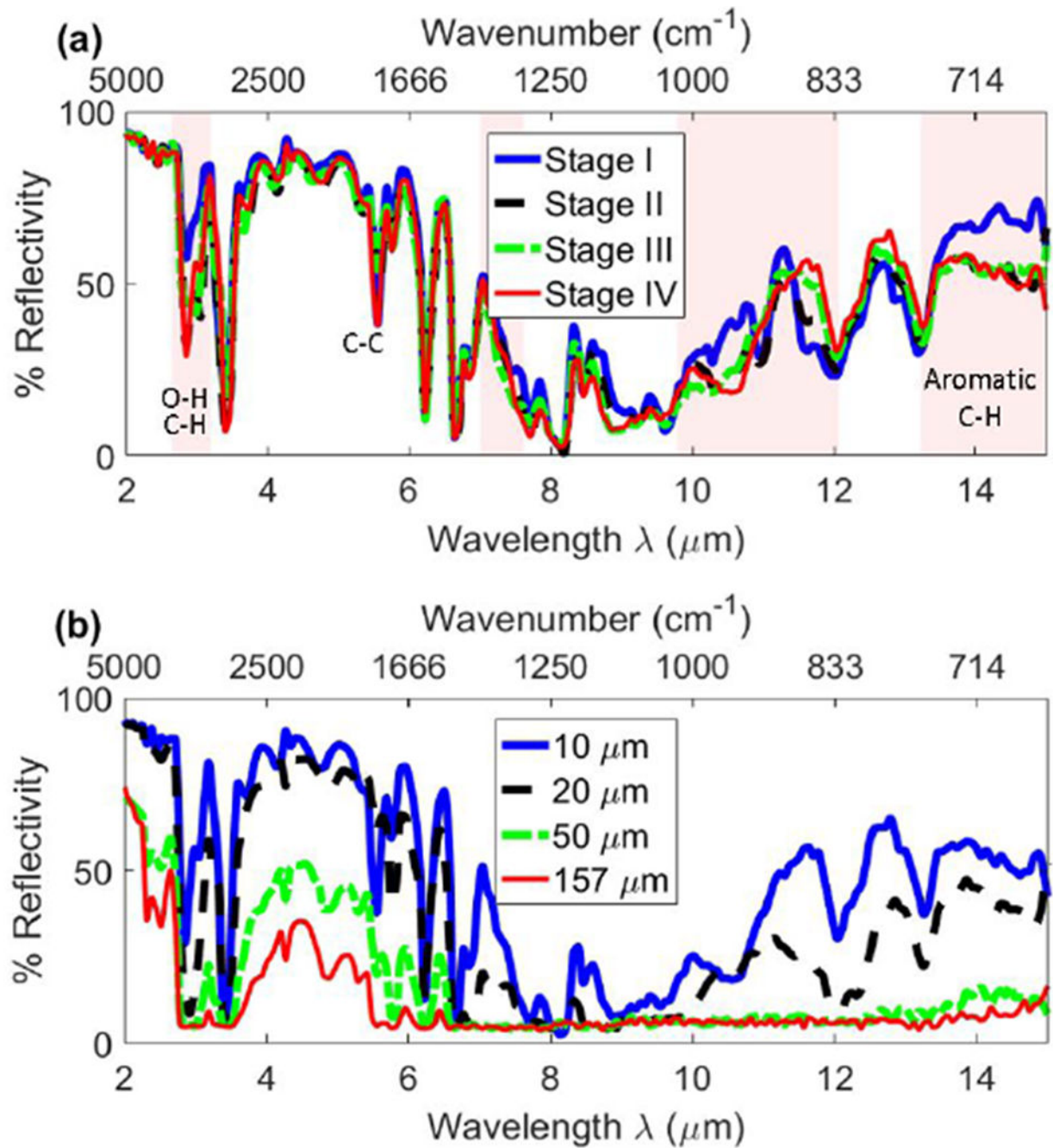


**Fig. 2.**

(a) Effect on reflectance spectrum after each treatment step on the  $10 \mu\text{m}$  sample of SU-8; stage I: soft baking, stage II: UV exposure, stage III: post-exposure bake and stage IV: hard bake. Shaded region highlights wavelengths at which a significant change in reflectance is seen. (b) Measured reflectance of UV and heat treated SU-8 samples with various film thicknesses.

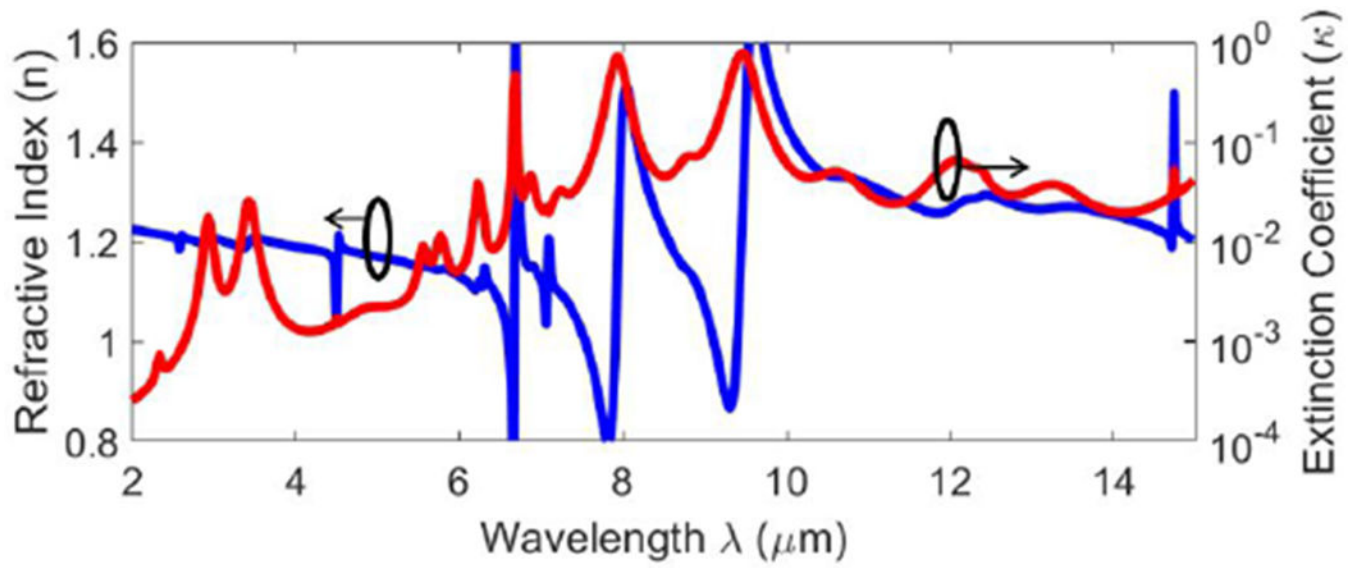


**Fig. 3.**  
Estimated refractive indices of UV treated SU-8

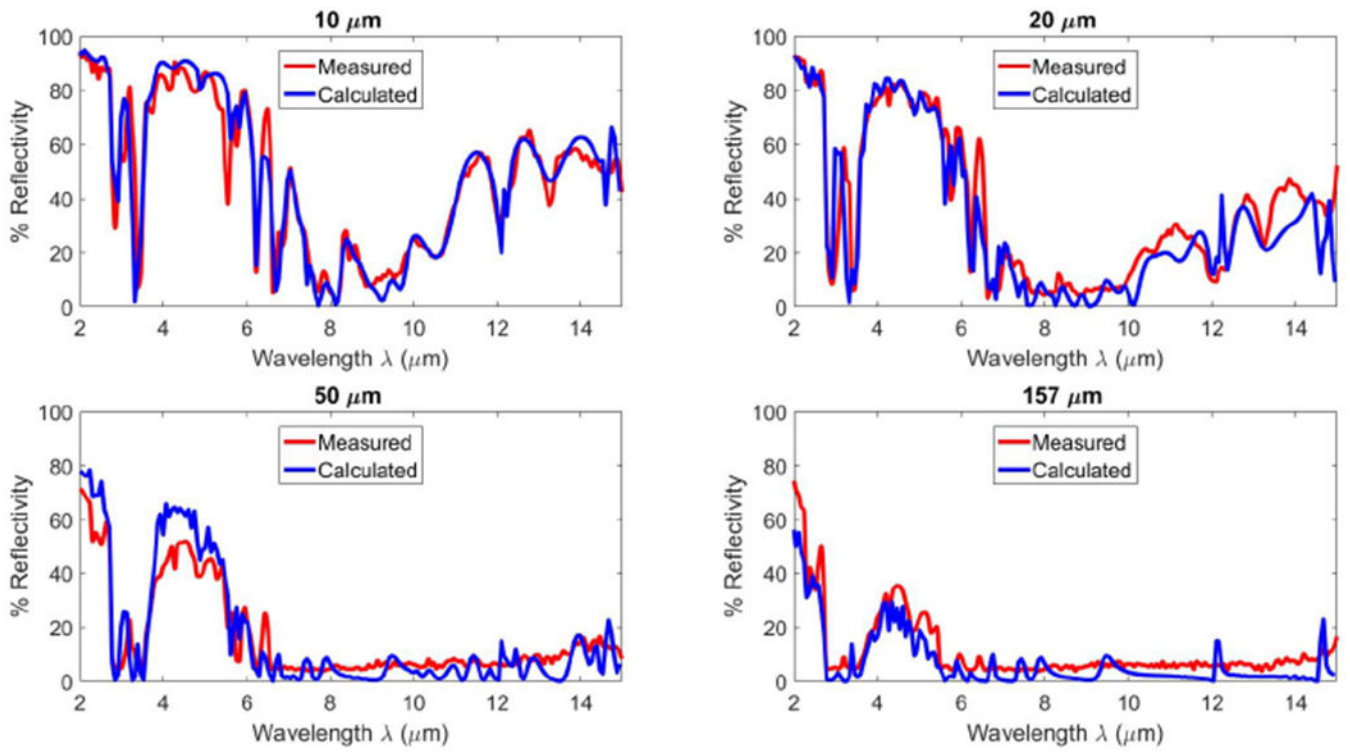


**Fig. 4.** Comparison of measured and calculated reflectance of UV treated SU-8 samples with different thickness.

**Table 1.**

Lorentz-Drude oscillator parameters of SU-8 after UV and heat treatment

k -	$\omega_k$ (cm <sup>-1</sup> )	$\lambda_k$ ( $\mu$ m)	$s_k$ -	$\Gamma_k$ -	Vibrational Bond
1	3469	2.9	5.379E-04	1.198E-02	O-H
2	2955	3.4	1.474E-02	2.654E-03	Aliphatic C-H
3	1768	5.7	1.345E-03	2.151E-04	
4	1702	5.9	4.714E-03	2.520E-05	Aromatic C-C
5	1610	6.2	2.330E-03	2.242E-04	
6	1599	6.3	1.138E-03	1.100E-01	
7	1479	6.8	6.422E-03	1.928E-03	
8	1344	7.4	3.731E-04	4.898E-05	
9	1339	7.5	9.896E-03	8.090E-05	
10	1265	7.9	2.033E-02	1.242E-02	
11	1227	8.2	1.944E-03	2.234E-02	
12	1067	9.4	3.227E-02	1.668E-02	
13	947	10.6	3.071E-03	3.863E-02	
14	831	12.0	3.412E-03	4.090E-02	
15	823	12.1	5.759E-03	3.790E-05	
16	757	13.2	3.073E-03	3.831E-02	Aromatic C-H (out of plane)
17	682	14.7	5.168E-03	5.400E-05	
18	648	15.4	6.622E-03	2.668E-02	Aromatic C-C (out of plane)

$$\epsilon_{\infty} = 1.4$$

**Table 2.**

Lorentz-Drude oscillator parameters of SU-8 before UV exposure

k -	$\omega_k$ (cm <sup>-1</sup> )	$\lambda_k$ ( $\mu$ m)	$s_k$ -	$\Gamma_k$ -	Vibrational Bond
1	3459	2.9	5.288E-04	1.633E-02	O-H
2	2963	3.4	1.615E-02	2.009E-03	Aliphatic C-H
3	1766	5.7	1.101E-03	1.195E-04	
6	1727	5.8	9.321E-04	1.500E-01	Aromatic C-C
4	1702	5.9	4.727E-03	1.630E-05	
5	1611	6.2	2.569E-03	3.018E-04	
7	1480	6.8	7.252E-03	2.295E-03	
8	1344	7.4	2.120E-04	3.086E-05	
9	1338	7.5	9.496E-03	3.953E-05	
10	1267	7.9	2.267E-02	1.143E-02	
11	1180	8.5	9.107E-04	1.241E-02	
12	1055	9.5	2.862E-02	1.448E-02	
13	938	10.7	1.886E-03	4.126E-02	
14	836	12.0	4.794E-03	3.526E-02	
15	823	12.1	5.726E-03	4.452E-05	
16	760	13.2	2.895E-03	2.617E-02	Aromatic C-H (out of plane)
17	682	14.7	5.220E-03	3.001E-05	
18	642	15.6	6.403E-03	3.637E-02	Aromatic C-C (out of plane)

$$\epsilon_{\infty} = 1.4$$